Structure and Function of Wool Keratin Polypeptide Extracted by Superheated Water

by

Ting Wu,[a, b] Min He,[a, b] Wenhua Yang,[a, b] Zhihua Shan,[a, b] Hui Chen[a, b,*]

[a]*College of Biomass Science and Engineering, Sichuan University,* Chengdu, 610065, China

[b]*The Key Laboratory of Leather Chemistry and Engineering (Sichuan University), Ministry of Education,* Chengdu, 610065, China

Abstract

Pyrohydrolytic wool keratin polypeptides (PWKPs) were successfully extracted by hydrolyzing waste sheep wool from a tannery with superheated water. The results revealed that the properties of PWKPs varied significantly under different hydrolysis temperatures. At 170°C, the weight average molecular weight and the polydispersion index of the product PWKP-170 were determined to be 1080 ± 71 Da and 1.55 ± 0.04, respectively, which displayed a distribution trend for "equilong chain segments". Furthermore, the extraction yield and the repeated water solubility reached 93.5 ± 1.7% and 99.8 ± 0.2%, respectively, and no α-helical structure was found to exist in PWKP-170. Organic element and amino acid analyses for the PWKPs showed that the decrease in sulfur and cysteine content was related to the fracture of disulfide bonds during the hydrolysis process of keratin. Specificity studies indicated that PWKP-170 exhibited a new ultraviolet absorption characteristic at 309 nm, with an antibacterial titer of 11.24 AU/mg against Staphylococcus aureus at a concentration of 1×10^6 CFU/mL, reflecting its potential application value as a keratin polypeptide functional material.

Introduction

It has been reported that the annual output of waste animal hair reaches up to 1.43×10^5 t in the global leather industries.[1] As a major country for leather and fur manufacturing, China produces more than 7×10^7 pieces of bovine hide and 1×10^8 pieces of sheep skin each year. Therefore, a large amount of bovine hair and wool needs to be disposed. At present, although part of waste hair is processed into felt, landfill is still regarded as the main disposal method, resulting in a waste of resources and requiring much soil space.[2] At the same time, there exists a risk of spongiform encephalopathy with this treatment. Hence, the recycling of wastes has become an inevitable trend of industrial development. The extraction of keratin polypeptide from waste hair is deemed an important approach to realize resource utilization.[3-5] The extraction mechanism lies in the destruction of disulfide bonds and amide bonds, which leads to the hydrolyzation of highly crosslinked and water-insoluble keratin into polypeptides with a small molecular weight and good water solubility.

The diversified extraction methods for keratin polypeptide include chemical hydrolysis, biological hydrolysis and physical hydrolysis. Chemical hydrolysis exhibits a high yield and a low requirement for procedure parameters, generally at a temperature of at most 100°C and normal atmospheric pressure. Nevertheless, the product needs to be purified several times to remove residual reagents, which induces breakage of the structural integrity, waste of water and environmental pollution.[6-8] For biological hydrolysis, no or a small number of chemical reagents are adopted under mild conditions. This method entirely depends on the performance of microorganisms or enzymes and requires high control for condition parameters with a low yield. Moreover, most keratinases belong to the excision enzyme, leading to the end product to be composed of free amino acids, with the difficult control of the molecular weight.[4, 9] To date, there are no reports that keratinase hydrolysis can be used to obtain a material with a specific molecular weight or a characteristic property on the premise of guaranteeing the extraction yield. For physical hydrolysis, a highly pure product can be fabricated by means of simple separation, such as filtration or centrifugation, with a low post-treatment cost. Furthermore, the sample is highly water-soluble under neutral conditions (especially superheated water hydrolysis). In contrast, from an environmental point of view, superheated water hydrolysis is more suitable for the recovery of keratin polypeptide from waste hair.[10-12]

Superheated water hydrolysis (SHWH) refers to the process during which the tissue structures of keratin are hydrolyzed under high temperature and high pressure for a certain time. Parag S. Bhavsar et al.[13,14] treated unwashed wool at 170°C for 60-90 min to complete partial hydrolysis by SHWH. The results showed that the molecular weight of the material varied from 600 Da to 1400 Da, the cysteine content decreased by 94.3%, and the C/N ratio declined from 4.26 to 3.55. A wheat germination experiment indicated that wool keratin polypeptide exhibited no toxic side effects and promoted the growth of wheat. M. Zoccola et al.[15] studied the influence of wool keratin polypeptide as a slow-release nitrogen fertilizer on the growth of grass by measuring the variation in the organic element content. The analysis suggested that the utilization of polypeptides reduced fertilizer usage compared to traditional chemical fertilizers in pasture lands and enhanced the carbon sequestration rate, which showed the potential agricultural application value of wool keratin

*Corresponding author email: chenh@scu.edu.cn

Manuscript received March 1, 2022, accepted for publication April 27, 2022.

polypeptide. Parag S. Bhavsar et al.[16] also applied wool keratin polypeptide extracted by SHWH at 170°C to a foaming agent. In the dyeing process of cotton and woolen fabrics with reactive and acid dyes, the sample exhibited a comparable effect to that of conventional dyeing auxiliaries, thus reducing the load on the effluent. However, there is still a lack of insights into the extraction of wool keratin polypeptide by SHWH. As a byproduct of the leather industry, waste hair has significant potential for recycling. Nevertheless, owing to the special physical structure of animal hair and the heterogeneity of the keratin chemical structure, a complete and in-depth performance characterization of the product should be investigated. Therefore, it is extremely urgent to explore multiple approaches to the functional development of keratin polypeptides extracted through environmentally friendly SHWH, which will lay a foundation for the construction of featured functional materials and realize the green high-value conversion of leather waste wool.

Among all the sources of waste animal hair, the waste sheep wool from the shearing factory, tannery and textile mill exhibits a high extraction value for keratin polypeptide due to the absence of pigments and fewer surface impurities. Hence, the raw material in this experiment was obtained from waste sheep wool manually pushed by a sheep leather processing enterprise. In this work, keratin polypeptide was extracted from clean waste sheep wool by using an optimized SHWH scheme. The solubility and the chemical structure of the samples were analyzed, and the ultraviolet absorption and bacteriostatic properties of the degradation product solutions were characterized, which can offer further support for the preparation of natural high-quality biological material from waste wool keratin polypeptide.

Experimental section

Main materials

Staphylococcus aureus *CMCC (B) 26003*, Bacillus subtilis *CMCC (B) 63501*, Pseudomonas aeruginosa *CMCC (B) 10104*, Escherichia coli *CMCC (B) 44102*, Aspergillus niger *CMCC (F) 98003*, Candida albicans *CMCC (F) 98001*, peptone, beef powder, agar, potato powder and glucose were purchased from Zhangzhou Seymour Biotechnology Co., Ltd. (China). All reagents were of biological grade and used as received.

Optimization of PWKP extracted by SHWH

Extraction yield

Approximately 10 g of waste sheep wool crushed to 5-10 mm long segments was degreased by shaking in 50 g of deionized water with 0.1 g of sodium dodecyl benzene sulfonate and 0.2 g of sodium carbonate at 45°C for 1 h. The degreasing fluid was drained, and then 0.5 g of peroxide and 50 g of distilled water were added, followed by stirring at 45°C for 1 h. The liquid was drained and the treated wool was dried to obtain the raw material wool for SHWH.[17] The wool and distilled water were mixed at a certain mass ratio in a 150 mL hydrothermal reaction kettle (Yikai, China) and heated under a specified temperature and time. After that, the hydrolysate was filtered through a microfiltration membrane, and then the filtrate was freeze-dried at -50°C to prepare the pyrohydrolytic wool keratin polypeptide (PWKP). The extraction yield (R) for PWKP was calculated according to Eq. (1).

$$R = \frac{m_2}{m_1} \times 100\% \quad (1)$$

where m_1 is the weight of the wool and m_2 is the weight of PWKP.

Single-factor experiment

During the course of extracting PWKP by SHWH, R is used as a primary evaluation indicator. Therefore, single-factor experiments were conducted to investigate the influence of hydrolysis temperature (T = 150-190°C), wool mass fraction (w = 5-25%) and hydrolysis time (t = 1-5 h) on R and to obtain the optimal factors (T_o, w_o, t_o). Based on previous reports,[14, 18] the basic hydrolysis conditions were set as T = 170°C, w = 10% and t = 2 h. In order of (T, w, t), the optimal temperature was obtained first, followed by dosage, and finally time.

Preparation of PWKP

According to the experimental results (T_o, w_o, t_o) acquired from above, wool was hydrolyzed under three hydrolysis conditions at different temperatures (T_{o1}, w_o, t_o), (T_{o2}, w_o, t_o) and (T_{o3}, w_o, t_o). Subsequently, the hydrolysate was dialyzed with distilled water at 4°C for 8 h to remove inorganic salts. Finally, the dialysate was freeze-dried to prepare PWKP-T_{o1}, PWKP-T_{o2} and PWKP-T_{o3}. All of the above samples were collectively labeled PWKPs.

Characterization

The relative molecular weight parameters of the PWKPs were detected using an RID-20 differential refractive index detector (Shimadzu, Japan) equipped with a TSK-gel GMPWXL aqueous gel permeation chromatography (GPC) column (TOSOH, Japan). The mobile phase consisted of 0.1 mol/L $NaNO_3$ and 0.05% NaN_3 aqueous solution. The flow rate and the column temperature were maintained at 0.6 mL/min and 35°C, respectively. PWKP was added to distilled water and then magnetically stirred at 25°C for 10 min, followed by filtering. Then, the filtrate was freeze-dried at -50°C. The repeated water solubility (R_{re}) of the PWKP was calculated using Eq. (2).

$$R_{re} = \frac{m_2}{m_1} \times 100\% \quad (2)$$

where m_1 is the weight of the PWKP and m_2 is the weight of the water-soluble part of the PWKP. X-ray diffraction (XRD) patterns for wool and PWKPs were characterized using an Empyrean X-ray diffractometer (Panalytical, Holland). The generator voltage and the tube current were 40 kV and 40 mA, respectively. The scanning range was 5-60° and the step size was 0.02°.

Composition characterization

The organic element content of the wool and PWKPs was analyzed using an EL cube elemental analyzer (Elementar, Germany). A total of 0.1 g of the sample was fully dissolved in an ampoule bottle containing 5 mL of HCl solution (6 mol/L), and then N_2 was continuously injected into the bottle for 10 min. Subsequently, the digestion reaction was carried out at 110°C for 24 h. After that, the digestion solution was dried at 60°C, and then the residues were dissolved with 5 mL of a Tris-HCl buffer solution (pH = 7.4), followed by filtering. Finally, the amino acid compositions of the filtrate for the wool and PWKPs were determined using an L-8900 amino acid analyzer (Hitachi, Japan).

The size and temperature of the ion exchange column equipped with a 2622 ion exchange resin (Hitachi, Japan) were 4.6 × 60 mm and 57°C, respectively. The reaction column contained an 855-3523 quartz sand (Hitachi, Japan) with a size of 4.6 × 40 mm and a temperature of 135°C. The flow rates for the ninhydrin and buffer solutions were 0.35 mL/min and 0.4 mL/min, respectively. The injection volume was 20 μL and the detection wavelength was 570 nm. The cycle time and the collection time were 20 min and 10 min, respectively. In addition, based on the amino acid compositions of wool, the reference sample (RS) was prepared with analytical pure amino acids for subsequent experiments.

Absorption characterization

Fourier transform infrared (FT-IR) spectra for the wool, PWKPs and RS were recorded using a Nicolet iS10 Fourier transform infrared spectrometer (Thermo Scientific, USA). Each sample was analyzed from 500 cm^{-1} to 4000 cm^{-1}. Ultraviolet–visible (UV-Vis) absorption characterization for the PWKPs and RS was conducted using a UV-3100 ultraviolet–visible spectrophotometer (Mapada, China). The wavelength range was 250-450 nm and the step size was 1 nm.

Bacteriostasis characterization

Qualitative bacteriostasis characterization

According to the experimental data of R_{re}, the bacteriostatic activity of PWKP, which was observed to be completely water-soluble under neutral conditions, was qualitatively characterized based on the inhibition zone diameter with filter paper. Gram-positive bacteria (Staphylococcus aureus *CMCC (B) 26003*, Bacillus subtilis *CMCC (B) 63501*) and gram-negative bacteria (Pseudomonas aeruginosa *CMCC (B) 10104*, Escherichia coli *CMCC (B) 44102*) were cultured in nutrient agar media, while potato glucose agar media were used for fungi (Aspergillus niger *CMCC (F) 98003*, Candida albicans *CMCC (F) 98001*). The specific experimental procedures are described below.

A certain number of second-generation inclined bacteria were placed into the PBS buffer solution to form the initial bacterial suspension with a concentration of approximately 1 × 10^8 CFU/mL. The suspension concentration was diluted to 1 × 10^6 CFU/mL with buffer solution to prepare the inoculative bacterial suspension. Then, 0.5 mL of the inoculative bacterial suspension was evenly spread over the culture dish containing the culture medium. After 20 min, five standard filter papers with a thickness of 1 mm and a diameter of 6 mm were placed into the dish at intervals of 2.0-2.5 cm. Then, 20 μL of the PWKP solution with different concentrations of 1.0 mg/mL, 3.0 mg/mL, 5.0 mg/mL, 7.0 mg/mL and 10.0 mg/mL was dropped onto the center of each filter paper. Subsequently, the dish was transferred to a 37°C incubator for 24 h to observe the inhibition zone around the filter paper. The inhibition zone diameter (*IZD*) was measured along three directions with a Vernier caliper, and the bacterium on which the PWKP showed the best bacteriostatic effect and the corresponding minimum inhibition concentration (ρ_{min}) were determined for quantitative bacteriostasis characterization.

Quantitative bacteriostasis characterization

Quantitative bacteriostasis characterization of PWKP was performed according to GB/T 39101-2020. Twenty milliliters of the culture medium and 0.2 mL of the inoculative bacterial suspension were homogeneously mixed in a sterilized glass culture dish, followed by solidification at 4°C. After that, five Oxford cups filled with 100 μL of the PWKP solution with different concentrations (ρ_{pwkp}) of $1\rho_{min}$, $2\rho_{min}$, $4\rho_{min}$, $8\rho_{min}$ and $16\rho_{min}$ mg/mL were placed into the dish at intervals. Subsequently, the dish was placed at 4°C for 10 h to ensure the adequate diffusion of PWKP and then transferred to a 37°C incubator for 24 h. The linear fitting curve was established with the negative logarithm of the dilution multiple (n) of ρ_{pwkp} relative to $16\rho_{min}$ as the abscissa and *IZD* as the ordinate. The antibacterial titer (U, AU/mg) of PWKP was calculated using Eq. (3).

$$U = \frac{1}{V \times 10^{X_0} \times 16\rho_{min}} \quad (3)$$

where V is the volume of the PWKP solution and X_0 is the X-intercept of the linear fitting curve.

Results and discussion

Single-factor SHWH experiment analysis

The influence of hydrolysis temperature (T), wool mass fraction (w) and hydrolysis time (t) on R is shown in Table I. It can be found that R markedly increased with increasing T and reached a value of 93.5 ± 1.7% at 170°C. When T exceeded 170°C, R was increased by only 1.4% at 180°C and 2.0% at 190°C. Minor distinctions existed among R in a w range of 5-20%, and R dropped down to 90.9 ± 2.5% when w was raised to 25%. As shown in Table I, R was gradually enhanced with increasing t and reached a value of 95.4 ± 1.9% when wool was hydrolyzed for 3 h, whereas little change occurred after 3 h.

In summary, the single-factor experimental results indicated that the optimal factors were T_o = 170°C, w_o = 20% and t_o = 3 h. On

Table I

The influence of *T*, *w* and *t* on R.

T/°C	150	160	170	180	190
R/%	52.1 ± 1.1	75.4 ± 1.5	93.5 ± 1.7	94.9 ± 1.3	95.5 ± 0.8
w/%	5	10	15	20	25
R/%	95.8 ± 1.2	95.1 ± 1.1	94.9 ± 1.7	95.1 ± 2.1	90.9 ± 2.5
t/h	1	2	3	4	5
R/%	83.2 ± 3.1	91.5 ± 1.5	95.4 ± 1.9	95.5 ± 1.3	95.6 ± 0.9

this basis, raising *T*, reducing *w* and prolonging *t* contributed to improving *R*, but the effects were not evident. Moreover, it was noteworthy that *T* exhibited the most significant influence on *R*. When *T* reached 150°C, *R* was equal to 52.1 ± 1.1%, lower than the data reported for alkaline hydrolysis[19] and higher than that for microwave-assisted SHWH.[11] The *R* value of 75.4 ± 1.5% at 160°C was similar to the result obtained from peracetic acid hydrolysis[8] and greater than that from microwave-assisted SHWH. When *T* was increased to 170°C, *R* reached up to 93.5 ± 1.7%, which was basically the same as that for alkaline hydrolysis. Therefore, the hydrolysis temperatures for further experiments were determined to be T_{o1} = 150°C, T_{o2} = 160°C and T_{o3} = 170°C, and the corresponding products were coded as PWKP-150, PWKP-160 and PWKP-170, respectively.

GPC analysis

As shown in Fig. 1A, the weight average molecular weight (M_w) ranged from 9568 ± 241 Da to 1080 ± 71 Da with much difference. The results indicated that the relative molecular weight of PWKP was highly correlated with *T*, and the macromolecular chain segment dominated PWKP at low hydrolysis temperatures. However, it has been reported that the M_w of alkaline hydrolyzed wool keratin polypeptide was concentrated in the range of 800-1000 Da at the same temperatures,[14] demonstrating the relatively centralized molecular weight distribution and lower number of macromolecular chain segments. The above phenomena revealed that the mechanisms for the two hydrolysis methods were different. In addition, the polydispersion index (*PDI*) can also reflect the distribution characteristic of the molecular weight. The *PDI* values for PWKP-150 and PWKP-160 were determined to be 3.62 ± 0.14 and 2.90 ± 0.14, respectively, which meant that each molecule in the same sample showed a great variation in molecular weight. The *PDI* of PWKP-170 was determined to be 1.55 ± 0.04 with a minor discrepancy between M_w and number average molecular weight (M_n), proving that when *T* was increased to a certain level, the molecular weight distribution of PWKP tended to become uniform, that is, the "equilong chain segments" tendency. Consequently, the molecular weight of wool keratin polypeptide could be concentrated at approximately 1000 Da by SHWH with a hydrolysis temperature of 170°C, which was similar to that obtained in earlier work.[11]

Repeated water solubility analysis

After wool was hydrolyzed with superheated water, the hydrolysate displayed a colloid solution composed of wool keratin polypeptide and water, which belonged to a thermodynamic dispersion system with poor stability. Under certain conditions, the disulfide bonds, which were broken during the hydrolysis process for wool, had the ability to self-heal and thus started aggregating back. Hence, self-aggregation behavior might occur through dynamic covalent interactions of disulfide bonds, inducing the appearance of sediments or suspended particles. Furthermore, during the drying

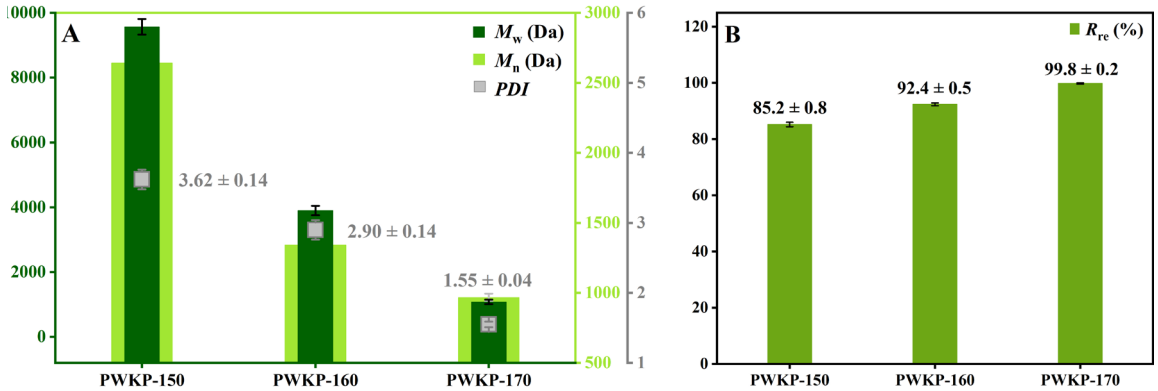

Figure 1. (A) Relative molecular weight parameters and **(B)** repeated water solubilities of PWKPs.

process, molecules contacted each other with the disappearance of hydration layers, leading to a greater likelihood of generating hydrophobic aggregations, and, thus, the formation of a water-insoluble product. Therefore, the repeated water solubility (R_{re}) should be considered to expand the further applications of PWKP. It can be seen in Fig. 1B that the R_{re} values of PWKP-150, PWKP-160 and PWKP-170 were 85.2 ± 0.8%, 92.4 ± 0.5% and 99.8 ± 0.2%, respectively, which meant that only PWKP-170 could be completely dissolved in water under neutral conditions. Apart from that, in combination with the experimental GPC data, the molecular weight of PWKP gradually declined with increasing *T*, giving rise to an increase in R_{re}. The results proved a definite relation between the molecular weight and R_{re} of PWKP. This was because that larger molecular weight meant longer chain length with more hydrophobic region compared to hydrophilic region, which led to PWKP being less water-soluble.

XRD analysis

Fig. 2A displays the XRD patterns for wool and PWKPs. For wool, PWKP-150 and PWKP-160, the two wide diffraction peaks were located at 9.1° and 20°, respectively, which were attributed to the α-helix and β-fold of keratin.[20] Nevertheless, a peak at 9.1° was not detected in PWKP-170. This result indicated that there was no α-helix in PWKP-170, whereas the β-folded structure still existed. It also revealed that when *T* was increased to 170°C, the α-helical structures of wool were completely damaged, which was consistent with other research findings.[11, 14, 18]

Organic element content analysis

Fig. 2B shows the organic element contents of wool and PWKPs. The C, N, H and S content changed before and after hydrolysis. With increasing *T*, *w*(C) and *w*(S) decreased while *w*(N) and *w*(H) increased. Except for S, the fluctuations in the other element contents were not significant. The *w*(S) values decreased from 3.87% to 2.16%, 2.07% and 1.68% as *T* was increased to 150°C, 160°C and 170°C, respectively. This phenomenon could be explained by the fact that the S element in wool principally existed in cystine in the form of a disulfide bond (—S—S—), and the disulfide bonds were broken during the hydrolysis process for wool, leading to a dramatic decrease in *w*(S). With regard to PWKP-170, *w*(S) was reduced by more than 50% compared with wool. The result indicated that the disulfide bonds of wool were adequately hydrolyzed in PWKP-170, inducing a smaller molecular weight, a better repeated water solubility and a lower *w*(S).

Amino acid composition analysis

Table II presents the amino acid compositions of wool and PWKPs. The most evident variation appeared in cysteine (Cys). The Cys content of wool was 10.30%, which was higher than that in the PWKPs. This was because during the acidic treatment process for amino acid composition characterization, many Cys residues were generated owing to the fracture of disulfide bonds, resulting in a greater Cys content in wool. For PWKP-150 and PWKP-160, the Cys contents were determined to be 3.55% and 1.12%, which represented a decrease of 65.5% and 89.1% in comparison with wool, suggesting that there were still some disulfide bonds left in the products. PWKP-170 possessed a lower Cys content of 0.52%, which was reduced by 95.0%, verifying that disulfide bonds were almost fully destroyed.[14] Moreover, the Cys residue could react with dehydroalanine to form lanthionine (Lant) or repolymerize to form cystine (Cya), inducing a dramatic decline in the Cys content and growth in the Lant and Cya contents of PWKPs.[13, 21]

For other amino acid contents, the reasons for the obvious fluctuations were speculated as follows. The hydrolysis of glutamine and asparagine led to the augmentation of the glutamic acid (Glu) and aspartic acid (Asp) contents. The decrease in tyrosine (Tyr) and threonine (Thr) contents resulted from the thermal oxidation of hydroxyl groups in the side chains at high temperatures. The reduction in lysine (Lys) and arginine (Arg) contents was ascribed to the destruction of side-chain alkaline groups at high temperatures. In general, the content of acidic groups (Glu and Asp) increased and that of alkaline groups (Lys and Arg) declined by SHWH. Furthermore, according to the amino acid composition of wool, the reference sample (RS) was prepared with analytical pure amino acids for subsequent characterization.

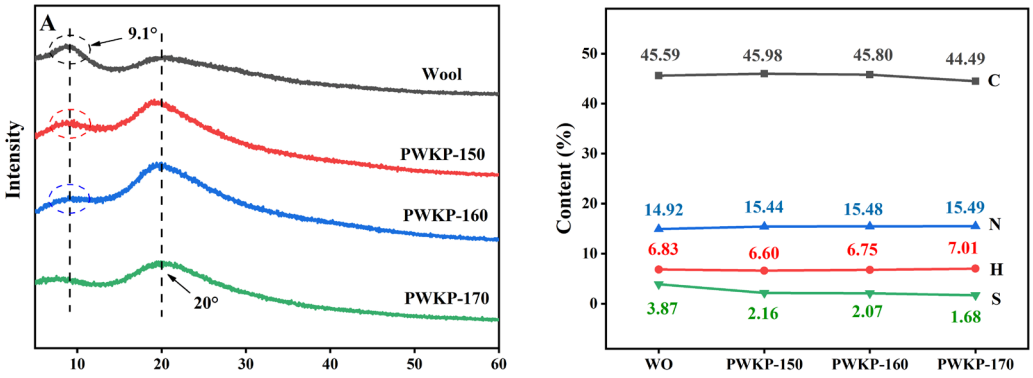

Figure 2. (A) XRD patterns and **(B)** organic element contents of wool and PWKPs.

Table II

Amino acid composition of wool and PWKPs.

Amino acid	Wool/mol%	PWKP-150/mol%	PWKP-160/mol%	PWKP-170/mol%
Cys	10.30	3.55	1.12	0.52
Lant	0.22	0.78	1.34	1.64
Cya	0.09	0.11	0.12	0.12
Glu	13.72	15.92	16.88	18.15
Asp	7.62	7.77	8.22	9.04
Tyr	3.09	2.88	2.55	2.50
Thr	6.03	5.77	5.26	5.09
Lys	3.42	3.35	3.21	3.01
Arg	6.73	6.58	6.16	5.44
Ser	10.39	10.13	9.34	9.12
Gly	7.89	8.46	9.25	9.90
His	0.62	0.63	0.67	0.69
Ala	5.23	5.97	6.77	7.33
Pro	5.71	5.93	6.23	6.44
Val	6.09	6.27	6.59	6.74
Met	0.38	0.39	0.39	0.40
Ile	3.20	3.30	3.36	3.46
Leu	7.15	7.46	7.67	7.88
Phe	2.21	2.11	1.94	1.86

FT-IR and UV-Vis absorption analysis

Fig. 3A displays the FT-IR spectra obtained for wool, PWKPs and RS. The wide absorption peak between 3000-3500 cm^{-1} was attributed to ν(N-H) and ν(O-H) of the amide band A.[22] The three absorption peaks between 2800-3000 cm^{-1} and the two peaks at 1400 cm^{-1} and 1450 cm^{-1} were ascribed to ν(C—H) of —CH_3 and —CH_2.[23] The peaks at 1650 cm^{-1} and 1540 cm^{-1} were assigned to ν(C=O) of amide band I[24] and ν(C—N) and δ(N—H) of amide band II,[21] respectively. The peak at 1240 cm^{-1} belonged to ν(C—N), ν(C—O), δ(N—H) and δ(O=C—H) of amide band III.[22] In addition, the absorption peaks at 1040 cm^{-1} and 1080 cm^{-1} were associated with ν(S-O).[21, 25, 26] Therefore, the absorption of PWKP-170 was not clear in this position. Moreover, it was worth noting that the absorption peak at 2570 cm^{-1} corresponding to ν(S—H) of the side chain of cysteine was visible only in RS,[27] demonstrating that wool and PWKPs contained no free cysteine residues. This was because that the cysteine residues may react with dehydroalanine to generate lanthionine or repolymerize to form cystine and so on.

Due to the conjugated double bond systems of phenylalanine, tryptophan and tyrosine, proteins possess obvious UV-Vis absorption characteristics. In the ultraviolet band, the absorption band can be divided into band R, band K, band B and band E. Among them, band R is formed by the lone pair electron transitions of chromophores, such as —C=O, —N=N— and —NO_2, which is located between 200-400 nm with a weak intensity. As shown in Fig. 3B, a wide absorption peak was located between 280-310 nm for PWKPs and RS. Nevertheless, unlike RS, a shoulder peak between 310-360 nm was detected in PWKPs. Fig. 3C shows the peak fitting curves for the PWKPs. The absorption spectra for the PWKPs were superposed by two curves with peak values of 288 nm and 309 nm. The emergence of a new absorption peak indicated the presence of functional groups capable of producing absorption in band R, such as —N=O and —NO_2. These functional groups were formed by the thermal oxidation of the —NH_2 of the side chains and the end groups in PWKPs. This also induced a solubility change from water-insoluble to water-soluble after oxidation for some keratins, which improved the extraction yield and the water solubility of the product under neutral conditions. In parallel, the absorbance of PWKP was enhanced with increasing *T* at the same wavelength because more chromophores and auxochromes were generated which made the product darker in color.

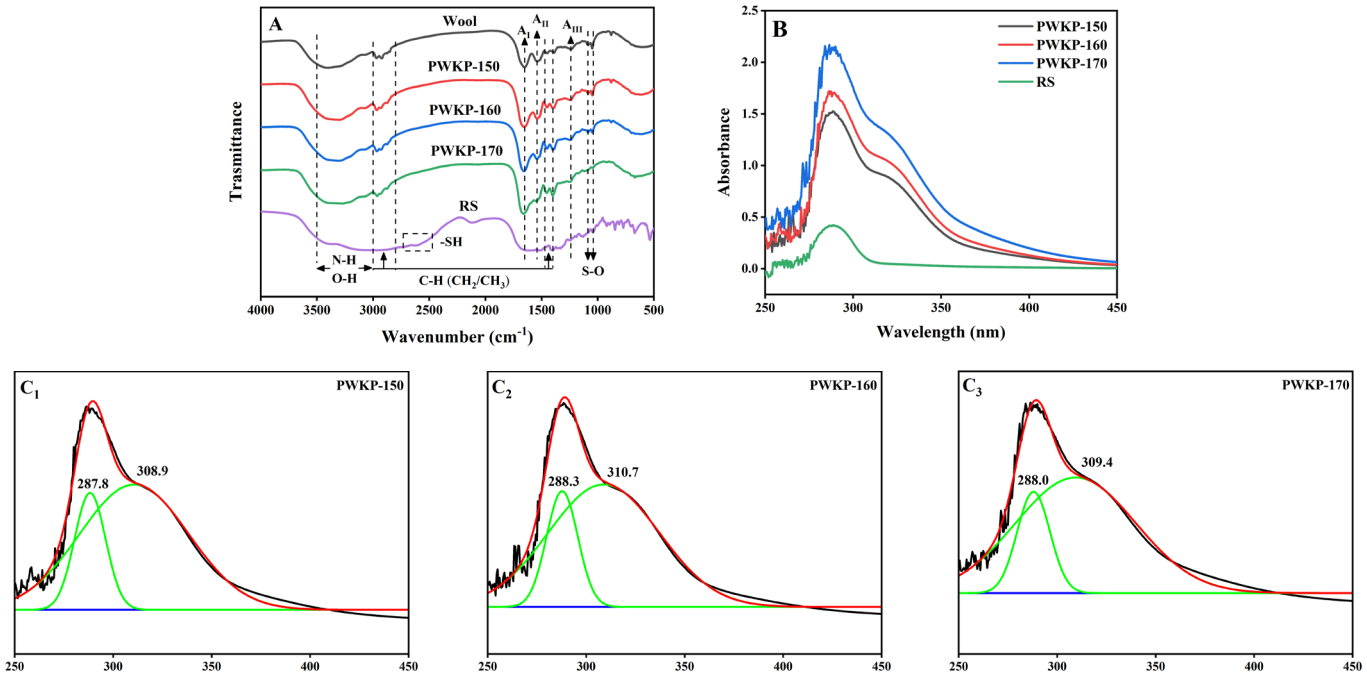

Figure 3. (A) FT-IR spectra for wool, PWKPs and RS; **(B)** UV-Vis spectra for PWKPs and RS; **(C)** Peak fitting curves for the UV-Vis spectra for the PWKPs.

Bacteriostasis analysis

Qualitative bacteriostasis analysis

In recent years, polypeptide compounds with bacteriostatic activity extracted from animals, plants and microorganisms have become a hot topic in the field of bacteriostatic drugs. At present, the widely recognized bacteriostatic mechanism is that polypeptides can bind to lipoteichoic acid in the bacterial cell membrane, leading to the destruction of the cell structure and eventually inhibition of bacterial growth.[28] According to the repeated water solubility acquired from above, only PWKP-170 could be completely dissolved in water under neutral conditions. Therefore, only PWKP-170 was selected for bacteriostasis characterization because of the neutral experimental conditions.

As shown in Fig. 4A, when the PWKP-170 concentration (ρ_{pwkp}) was kept in the range of 1.0-5.0 mg/mL, a clear growth boundary appeared at the edge of the filter paper in *Staphylococcus* aureus medium, whereas *IZD* expansion was not observed owing to the lower concentration. When ρ_{pwk} was increased to 7.0 mg/mL and 10.0 mg/mL, the *IZD* values reached up to 7.84 ± 0.48 mm and 9.98 ± 0.36 mm, respectively. Likewise, for *Bacillus subtilis medium*, *IZD* reached 6.43 ± 0.22 mm and 6.97 ± 0.34 mm when ρ_{pwk} exceeded 5.0 mg/mL. Nevertheless, no inhibition zones were observed around any filter papers in other media. This phenomenon suggested that when ρ_{pwk} grew to over 7.0 mg/mL, PWKP-170 exhibited a significant inhibition effect on the growth of *Staphylococcus aureus*, whereas it had a relatively weak bacteriostatic property for *Bacillus subtilis* and showed no bacteriostasis against *Pseudomonas aeruginosa, Escherichia coli, Aspergillus niger* and *Candida albicans*. Hence, it can be inferred that PWKP-170 possessed bacteriostatic activity against gram-positive bacteria but not against gram-negative bacteria and fungi. This was because of the structural difference between bacteria and fungi. The bacterial cell wall was composed of peptidoglycan,

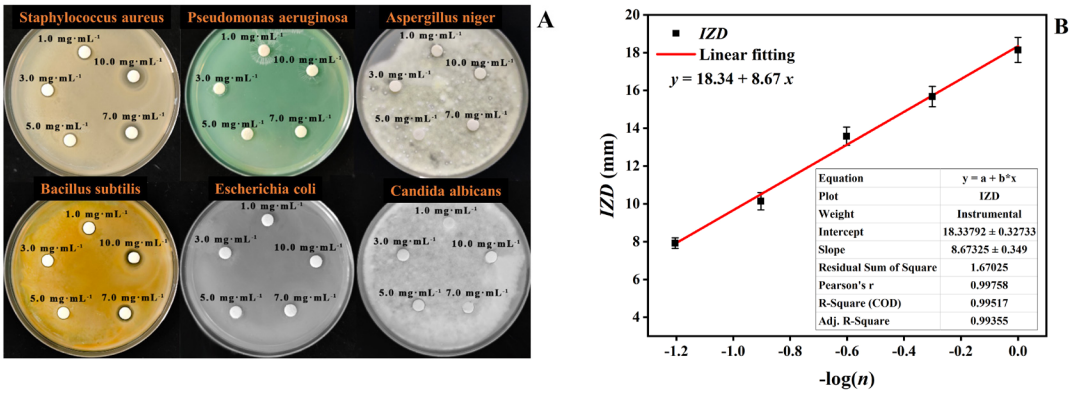

Figure. 4. **(A)** Optical images of the inhibition zones of PWKP-170 in different culture media; **(B)** Linear fitting curve for n and IZD for PWKP-170.

while the fungal cell wall consisted of chitosan. PWKP-170 could penetrate the cell walls of bacteria rather than fungi, rendering it ineffective against fungi. The discrepancy between gram-positive and gram-negative bacteria lied in the presence of lipoteichoic acids in gram-positive bacteria. Consequently, PWKP-170 had a bacteriostatic effect only on gram-positive bacteria.

However, there are different suggestions about the key functional structures and components of antibacterial peptides. Some scholars believe that the antibacterial activity originates from special amino acids, such as tryptophan, proline, arginine and cysteine.[29-31] Other researchers argue that the antibacterial property is derived from the amino acid content (such as hydrophobic amino acid content) and the special molecular structure (such as α-helix or special amino acid sequence fragment).[32] For PWKP-170, the bioactive structure and domain of keratin were destroyed after high-temperature treatment, and XRD analysis proved that no α-helical structure existed. As a consequence, the bioactive molecular structure may not play a contributing role in bacteriostasis. The bacteriostasis of PWKP-170 might be related to the specific amino acid or the amino acid composition ratio.

Quantitative bacteriostasis analysis

Based on the analytical results of 3.8.1, PWKP-170 showed the most evident bacteriostatic effect on *Staphylococcus aureus*, with a minimum inhibition concentration (ρ_{min}) of 7.0 mg/mL. Fig. 4B displays the linear fitting relationship between dilution multiple (*n*) and *IZD*. With a decrease in *n*, that is, with an increase in the PWKP-170 concentration, the *IZD* was gradually increased to 18.14 ± 0.66 mm. The formula of the fitting curve could be expressed as $y = 18.34 + 8.67\,x$ with an X-intercept of -2.11. According to Eq. (3), the antibacterial titer was calculated to be $U = 11.24$ AU/mg.

Conclusion

In this paper, waste sheep wool was hydrolyzed by superheated water, and then the hydrolysate was freeze-dried to prepare pyrohydrolytic wool keratin polypeptide (PWKP). The analytical results for organic element content and amino acid composition indicated that the degree of fracture of disulfide bonds varied with the hydrolysis temperature, which demonstrated a significant effect on the extraction yield, relative molecular weight and repeated water solubility. At 170°C, the product PWKP-170 exhibited excellent performance (R = 93.5 ± 1.7%, M_w = 1080 ± 71 Da, PDI = 1.55 ± 0.04 and R_{re} = 99.8 ± 0.2%). UV-Vis absorption and bacteriostasis experiments revealed that PWKP-170 showed a new UV absorption peak at 309 nm and a significant bacteriostasis to *Staphylococcus aureus*. The minimum inhibition concentration and the antibacterial titer of PWKP-170 were determined to be 7.0 mg/mL and 11.24 AU/mg, respectively, for *Staphylococcus aureus* at a concentration of 1×10^6 CFU/mL.

In summary, superheated water hydrolysis can achieve efficient hydrolysis for keratin and efficient extraction for polypeptide without the need for external chemical reagents, which is fully scalable with the current infrastructures and facilities. Based on the UV-Vis absorption property measured at a wavelength of 309 nm and the good digestibility of wool keratin polypeptide with a low molecular weight, PWKP-170 is intended to be an edible UV-resistant material. Furthermore, the significant bacteriostatic activity of PWKP-170 against *Staphylococcus aureus* indicates its potential application value in the bacteriostatic modification of medical foam. Therefore, it can be confirmed that PWKP-170, the hydrolysis product of waste wool from leather tanning, is a kind of natural intrinsic anti-ultraviolet and bacteriostatic polypeptide material that has potential for high-value applications. This work will provide new ideas for the recovery and utilization of leather waste wool resources.

Credit Authorship Contribution Statement

Ting Wu: Investigation, Methodology, Data curation, Writing-original draft. Min He: Data curation, Formal analysis. Wenhua Yang: Data curation, Formal analysis. Zhihua Shan: Visualization, Writing-review & editing. Hui Chen: Conceptualization, Methodology, Investigation, Writing-review & editing, Supervision.

Declaration of Competing Interest

The authors declare that they have no known competing financial interests or personal relationships that could have appeared to influence the work reported in this paper.

Acknowledgments

The research was supported by the Open Fund of Sichuan Province Cyclic Economy Research Center (No. XHJJ-2009) and the Sichuan University-Dazhou Municipal People's Government Strategic Cooperation Project (2021CDDZ-03).

References

1. Valeika, V., Širvaitytė, J., Bridžiuvienė, D., Švedienė, J.; An Application of Advanced Hair-Save Processes in Leather Industry as the Reason of Formation of Keratinous Waste: Few Peculiarities of its Utilisation. *ESPRI* **26**, 6223-6233, 2019.
2. Guo, J., Dai, R., Chen, H., Liang, Y., Shan, Z.H.; Research on the Composite and Functional Characteristics of Leather Fiber Mixed with Nitrile Rubber. *JLSE* **3**, 1-12, 2021.
3. de Souza, F.d.R., Benvenuti, J., Meyer, M., Wulf, H., Klüver, E., Gutterres, M.; Extraction of Keratin from Unhairing of Bovine Hide. *CEC* **209**, 118-126, 2020.

4. de Medeiros, I.P., Rozental, S., Costa, A.S., Macrae, A., Hagler, A.N., Ribeiro, J.R.A., Vermelho, A.B.; Biodegradation of Keratin by Trichosporum Loubieri RC-S6 Isolated from Tannery/Leather Waste. *IBB* **115**, 199-204, 2016.
5. Hussain, F.S., Memon, N., Khatri, Z., Memon, S.; Solid Waste-Derived Biodegradable Keratin Sponges for Removal of Chromium: A Circular Approach for Waste Management in Leather Industry. *ETI* **20**, 101120(1-13), 2020.
6. Zhang, C.H., Xia, L.J., Zhang, J.J., Liu, X., Xu, W.L.; Utilization of Waste Wool Fibers for Fabrication of Wool Powders and Keratin: A Review. *JLSE* **2**, 2020.
7. Ghosh, A., Clerens, S., Deb-Choudhury, S., Dyer, J.M.; Thermal Effects of Ionic Liquid Dissolution on the Structures and Properties of Regenerated Wool Keratin. *PDS* **108**, 108-115, 2014.
8. Shavandi, A., Carne, A., Bekhit, A.A., Bekhit, A.E-D.A; An Improved Method for Solubilisation of Wool Keratin Using Peracetic Acid. *JECE* **5**, 1977-1984, 2017.
9. Eslahi, N., Dadashian, F., Nejad, N.H.; An Investigation on Keratin Extraction from Wool and Feather Waste by Enzymatic Hydrolysis. *PBB* **43**, 624-648, 2013.
10. Li, Y.C., Guo, R.J., Lu. W.H., Zhu, D.Y.; Research Progress on Resource Utilization of Leather Solid Waste. *JLSE* **1**, 2019.
11. Zoccola, M., Aluigi, A., Patrucco, A., Vineis, C., Forlini, F., Locatelli, P., Sacchi, M.C., Tonin, C.; Microwave-Assisted Chemical-Free Hydrolysis of Wool Keratin. *TRJ* **82**, 2006-2018, 2012.
12. Chen, J.Y., Ding, S.Y., Ji, Y.M., Ding, J.Y., Yang, X.Y., Zou, M.H., Li, Z.L.; Microwave-Enhanced Hydrolysis of Poultry Feather to Produce Amino Acid. *CEPPI* **87**, 104-109, 2015.
13. Bhavsar. P.S., Zoccola, M., Patrucco, A., Montarsolo, A., Mossotti, R., Rovero, G., Giansetti, M., Tonin, C.; Superheated Water Hydrolysis of Waste Wool in a Semi-Industrial Reactor to Obtain Nitrogen Fertilizers. *ACS SCE* **4**, 6722-6731, 2016.
14. Bhavsar, P., Zoccola, M., Patrucco, A., Montarsolo, A., Rovero, G., Tonin, C.; Comparative Study on the Effects of Superheated Water and High Temperature Alkaline Hydrolysis on Wool Keratin. *TRJ* **87**, 1696-1705, 2016.
15. Zoccola, M., Montarsolo, A., Mossotti, R., Patrucco, A., Tonin, C.; Green Hydrolysis as an Emerging Technology to Turn Wool Waste into Organic Nitrogen Fertilizer. *WBV* **6**, 891-897, 2015.
16. Bhavsar, P.S., Zoccola, M., Patrucco, A., Montarsolo, A., Mossotti, R., Giansetti, M., Rovero, G., Maier, S.S., Muresan, A., Tonin, C.; Superheated Water Hydrolyzed Keratin: A New Application as a Foaming Agent in Foam Dyeing of Cotton and Wool Fabrics. *ACS SCE* **5**, 9150-9159, 2017.
17. Shu, C.H., Long, Z.Z., Chen, Z.J., Dai, R., Shan Z.H.; Rapid Improvement of Wool Keratin Fertiliser Efficiency Based on Electrodegradation. *SLTC* **106**, 83-89, 2022.
18. Sweetman, B.J.; The Hydrothermal Degradation of Wool Keratin. *TRJ* 37, 844-851, 1967.
19. Shavandi, A., Bekhit, A.E-D.A., Carne, A., Bekhit, A.; Evaluation of Keratin Extraction from Wool by Chemical Methods for Bio-Polymer Application. *JBCP* **32**, 163-177, 2016.
20. Goodings, A.C.; The Molecular Structure of Wool Keratin. *TRJ* 20, 454-466, 1950.
21. Rajabinejad, H., Zoccola, M., Patrucco, A., Montarsolo, A., Rovero, G., Tonin, C.; Physicochemical Properties of Keratin Extracted from Wool by Various Methods. *TRJ* **88**, 2415-2424, 2017.
22. Idris, A., Vijayaraghavan, R., Rana, U.A., Patti, A.F., MacFarlane, D.R.; Dissolution and Regeneration of Wool Keratin in Ionic Liquids. *GC* **16**, 2857-2864, 2014.
23. McGregor, B.A., Liu, X., Wang, X.G.; Comparisons of the Fourier Transform Infrared Spectra of Cashmere, Guard hair, Wool and other Animal Fibres. *JTI* **109**, 813-822, 2017.
24. Cardamone, J.M.; Investigating the Microstructure of Keratin Extracted from Wool: Peptide Sequence (MALDI-TOF/TOF) and Protein Conformation (FTIR). *JMS* **969**, 97-105, 2010.
25. Călin, M., Constantinescu-Aruxandei, D., Alexandrescu, E., Răut, I., Doni, M.B., Arsene, M-L., Oancea, F., Jecu, L., Lazăr, V.; Degradation of Keratin Substrates by Keratinolytic Fungi. *EJB* **28**, 101-112, 2017.
26. Gaidau, C., Epure, D-G., Enascuta, C.E., Carsote, C., Sendrea, C., Proietti, N., Chen, W.Y., Gu, H.B.; Wool Keratin Total Solubilisation for Recovery and Reintegration - An Ecological Approach. *JCP* **236**, 117586(1-12), 2019.
27. Manivannan, D., Kirubavathi, K., Bakiyaraj, G., Selvaraju, K.; Studies on L-Cystine Hydrobromide Single Crystals for Nonlinear Optical Applications. *JTUS* **12**, 64-68, 2018.
28. Chen, C.H., Lu, T.K.; Development and Challenges of Antimicrobial Peptides for Therapeutic Applications. *A(B)* 9, **24**(1-20), 2020.
29. Shelenkov, A., Slavokhotova, A., Odintsova, T.; Predicting Antimicrobial and Other Cysteine-Rich Peptides in 1267 Plant Transcriptomes. *A(B)* **9**, 60(1-8), 2020.
30. Feng, X.J., Jin, S.J., Wang, M., Pang, Q., Liu, C.L., Liu, R.Q., Wang, Y.J., Yang, H., Liu, F.J., Liu, Y.Y.; The Critical Role of Tryptophan in the Antimicrobial Activity and Cell Toxicity of the Duck Antimicrobial Peptide DCATH. *FM* **11**, 1146(1-14), 2020.
31. Mishra, A.K., Choi, J., Moon, E., Baek, K-H.; Tryptophan-Rich and Proline-Rich Antimicrobial Peptides. *M* 23, **815**(1-23), 2018.
32. Lorenzon, E.N., Piccoli, J.P., Santos-Filho, N.A., Cilli, E.M.; Dimerization of Antimicrobial Peptides: A Promising Strategy to Enhance Antimicrobial Peptide Activity. *PPL* **26**, 98-107, 2019.